Arab J Geosci (2017) 10:268
DOI 10.1007/s12517-017-3050-9

ORIGINAL PAPER

Airy's isostatic model: a proposal for a realistic case

Soumyajit Mukherjee[1]

Received: 7 March 2017 / Accepted: 25 May 2017

Abstract This work derives algebraic expressions for Airy-type isostatic equilibrium and disequilibrium of lithospheric blocks within asthenosphere, considering a more realistic case of continuously varying densities of the lithosphere along mutually perpendicular directions. Isostatic (dis)equilibrium must be linked to the porosity and density of the rock matrix, and to pore fluid density since these factors govern the bulk density of wet sediments/porous rocks. Two combinations of exponential and linear increase of density with depth are demonstrated. Isostatic disequilibrium would speed up sinking/uplift of the lithospheric blocks. Given any other (empirical) equations for density variation in three perpendicular directions, isostatic (dis)equilibrium such as Eqs. 14, 17, 18, 28, and 29 can be theorized as well.

Keywords Isostasy · Density-depth relation · Porosity · Pore fluid density · Rock matrix density

Introduction

> "Earth's surface processes, namely erosion, transport and sedimentation, tend to counteract… positive and negative vertical movements."—G.V. Bosch et al. (2016)

The leading isostasy models, such as that by Airy, consider lithospheric/crustal blocks with constant densities floating in the asthenosphere/mantle (Turcotte and Schubert 2002). However, even the same rock type usually gets denser as depth increases. Heterogeneity in density in lithosphere is common (Singh et al. 2015), and classically Airy model of isostasy has been modified by considering pressure exerted by individual layers of rocks of different densities: vide isostatic balance exercise for rifted basins in Turcotte and Schubert (2002). From a different perspective, Airy model was modified by Meinnesz by considering a distributed compensation region (Vanicek and Krakiwsky 1986). Litinsky (1989) formulated "effective density" for layered rocks that involve densities and thicknesses of each layers. Cordell (1973) suggested that density contrast decreases exponentially with depth, with decrement ranging from 0.3 to 1.5 c.c. km^{-1}. Density usually increases (Goteti et al. 2012) but rarely can even decrease (Ebbing et al. 2007 and its review) exponentially with depth. Carlson and Herrick (1990) stated an average density gradient of 0.32 Mg m^{-3} km^{-1}. Reid (1987) pointed out a linear increase in density with depth from oceanic crust. Such a linear relation has also been adopted/modeled for the entire lithosphere (e.g., Motavalli-Anbaran et al. 2013; Kumar et al. 2014; Xu et al. 2016), and sometimes specifically for the mantle (Clark and Ringwood 1964) that can depend on its thermal structure (Xu et al. 2016). Zhang and Chen (1992) referred such a relation from deep crust, which Hofmeister and Criss (2015) mentioned just as a possibility. Besides, density decreases in overpressure zones in marine and shallow sediments (Bowers 2001). Even soil layers may exhibit a similar density-depth relation (Román-Sánchez et al. 2017). The linear density-depth relation (e.g., Martinec and Fullea 2015) has also been incorporated in few tectonic models (Pearse and Bailey 2007). The linear relation could be ultimately guided by the temperature structure with depth (Nemčok 2016).

✉ Soumyajit Mukherjee
soumyajitm@gmail.com

[1] Department of Earth Sciences, Indian Institute of Technology Bombay, Powai, Mumbai, Maharashtra 400 076, India

Published online: 14 June 2017

Porous sedimentary rocks (clastics and carbonates; McCulloh 1967; Maxant 1980) might be filled up with pore fluids, usually water, and this modifies the depth integrated "mean density" (Goteti et al. 2012) of the lithospheric block. Layered sedimentary rocks undergoing deeper burial can compact more and show increase in density (Maden et al. 2015). A gradual variation in density can also be induced by metamorphism (review in Zhou 2009). Tenzer et al. (2012) derived for the entire Earth almost a linear density gradient of 13 ± 2 kg m^{-3} km^{-1} within the upper mantle, 6–58 km below the continental crust. A few geodynamic models have considered density variation in all the three directions (e.g., Zhou 2009). Goteti et al. (2012) used exponential depth-density relation of sediments in analytical models. Not all rocks increase density with depth, e.g., evaporate/rock salt where in fact the density falls slightly due to thermal expansion (Romer and Neugebauer 1991). Sedimentary facies variation in 2D is quite common in marine to non-marine transition zones where density of one rock type is expected to alter progressively into the other. The South Caspian Basin hosts the thickest (28 km: Knapp et al. 2007) known sediment pile on the Earth where linear density variation with depth persist up to a long distance/depth (Motavalli-Anbaran et al. 2013).

This work develops models of Airy type isostatic (dis)equilibrium of blocks with continuously varying densities in orthogonal directions. If someone picks up density of the surface rock as a representative of that of the entire lithosphere, she would be proceeding with unrealistic magnitude that is not representative of the lithosphere. The model presented here overcomes this problem. However, abrupt facies variation (Chaudhuri et al. 1987) along horizontal/vertical directions and depth-wise transition from crust to mantle (Fig. 3 of Xu et al. 2016), leading to sharp jump in density, may not be possible to fit with suitable empirical equations, and the model presented here does not work in those cases.

Model Consider a sedimentary lithospheric block floating on asthenosphere (Fig. 1). The block is porous and consists of a single phase fluid in the pore space (Rieke and Chilinganian 1974).

Here

$$\rho_{\mathrm{bw}} = \rho_{\mathrm{m}} - (\rho_{\mathrm{m}} - \rho_{\mathrm{f}})\varnothing \tag{1}$$

ρ_{bw}: wet bulk density of sediments/rock, ρ_{m}: matrix/mineral/grain density, ρ_{f}: fluid density, and $\varnothing$: fractional porosity.

If porosity falls exponentially with depth (Athy 1930):

$$\varnothing_z = \varnothing_0 \; e^{-bz} \tag{2}$$

$\varnothing_z$: porosity at depth z, $\varnothing_0$: porosity at surface (i.e., at $z = 0$), e: exponential series, and b: a constant. Note $b^{-1} = \lambda$: compaction constant.

From Eqs. 1 and 2,

$$\rho_{\mathrm{bwz}=} \rho_{\mathrm{m}-} (\rho_{\mathrm{m}-} \rho_{\mathrm{f}})\varnothing_0 \, e^{-bz} \tag{3}$$

This means, at surface, or

$$z = 0, \rho_{\mathrm{bw0}=}\rho_{\mathrm{m}-}(\rho_{\mathrm{m}-}\rho_{\mathrm{f}})\varnothing_0 \tag{4}$$

Case I This case shows density increases with depth (Z direction) exponentially. In two perpendicular horizontal directions X and Y, densities of two types of sediments/rocks vary linearly, which could be the case of a sedimentary facies variation. Lateral density variation has been inferred to affect rocks as deep as 20 km (Wu and Mereu 1990).

$$\rho(x, 0, 0) = \rho_{\mathrm{m}}-(\rho_{\mathrm{m}}-\rho_{\mathrm{f}})\varnothing_0 + k_x \, x \tag{5}$$

$$\rho\,(0, y, 0) = \rho_{\mathrm{m}}-(\rho_{\mathrm{m}}-\rho_{\mathrm{f}})\varnothing_0 + k_y \, y \tag{6}$$

$$\rho\,(0, 0, z) = \rho_{\mathrm{m}}-(\rho_{\mathrm{m}}-\rho_{\mathrm{f}})\varnothing_0 \, e^{-\mathrm{bz}} \tag{7}$$

Here, density gradients k_x, $k_y \neq 0$. Obviously for increase in density away from the origin (point O in Fig. 1), k_x, k_y, $b > 0$, and for the decreasing case, k_x, k_y, $b < 0$. Density at the origin is $\rho_{\mathrm{bw}} = \{\rho_{\mathrm{m}} - (\rho_{\mathrm{m}} - \rho_{\mathrm{f}})\,\varnothing_0\}$. From Eqs. 5 to 8, density at any point (x,y,z) within the block:

$$\rho(x, y, z) = \rho_{\mathrm{m}}-(\rho_{\mathrm{m}}-\rho_{\mathrm{f}})\varnothing_0 \, e^{-\mathrm{bz}} + k_x \, x + k_y \, y \tag{8}$$

Note that $\rho(x,0,0)$, $\rho(0,y,0)$, and $\rho(0,0,z)$ obtained from Eq. 8 match with Eqs. 5, 6, and 7, respectively.

Mass of the lithospheric block:

$$M = \int_0^{x_1}\int_0^{y_1}\int_0^{z_1} \rho_{\mathrm{bw}}(x, y, z)\; \mathrm{dx\; dy\; dz} \tag{9}$$

Equation 9 is a standard step adopted in finding mass of a body with variable density (e.g., Das and Mukherjee 1996).

Or

$$M = \int_0^{x_1}\int_0^{y_1}\int_0^{z_1} \left\{\rho_{\mathrm{m}-}(\rho_{\mathrm{m}-}\;\rho_{\mathrm{f}})\varnothing_0 e^{-bz} + k_x x + k_y y\right\}\mathrm{dx\; dy\; dz} \tag{10}$$

$$\text{Simplifying, } \mathrm{M} = \prod \mathrm{q_1}\left[\rho_{\mathrm{m}} + 0.5\left\{\mathrm{k_x x_1} + \mathrm{k_y y_1}\right\}\right] + (\rho_{\mathrm{m}-}\,\rho_{\mathrm{f}})\varnothing_0\,\mathrm{x_1 y_1 b^{-1}}\left(\mathrm{e^{-bz1}}-1\right) \tag{11}$$

Here, $q = (x, y, z)$. Thus, $\prod q_1 = x_1 y_1 z_1$

Volume of the block is $v = \prod \mathrm{q_1}$.

Therefore, the mean density (ρ_{e}) of the block:

$$\rho_{\mathrm{e}} = \left(\prod {q_1}^{-1}\, M\right) \tag{12}$$

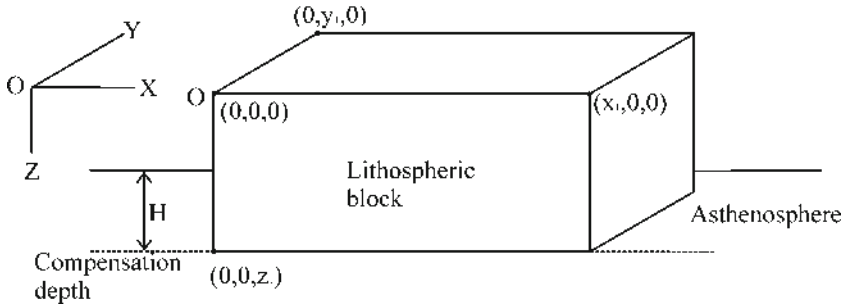

Fig. 1 A lithospheric block floating in asthenosphere. The compensation depth lies at the bottom surface of the block, as per the Airy model

which is

$$\rho_e = \left[\rho_m + 0.5\{k_x x_1 + k_y y_1\}\right] + (\rho_{m-}\ \rho_f)\varnothing_0\ z_1^{-1} b^{-1}\left(e^{-bz1}-1\right) \quad (13)$$

For isostatic equilibrium:

$$\rho_a\, H = z_1 \rho_e \quad (14)$$

Equation (14) is a standard way of pressure balance at the compensation depth (bottom margin of the lithosphere), as stated in pp. 74 of Turcotte and Schubert (2002).

For a constant rate of sedimentation $dz/dt = h_s > 0$, pressure difference per unit time driving the lithospheric block down:

$$d(\Delta P)\Big/dt = g\ \{h_s\ \rho_e - H\rho_a\} \quad (15)$$

g is the acceleration due to gravity. The rate of change of the force driving the block to sink

$$d(F_{down})\Big/dt = d(\Delta P)\Big/dt \times x_1 y_1 = g\ x_1 y_1\ \{h_s\ \rho_e - H\rho_a\} \quad (16)$$

"$x_1 y_1$" being the horizontal basal area of the block on which the force works.

Dividing this by the mass of the block as in Eq. 11, the rate of increase of acceleration of the sinking block:

$$d(f_{down})\Big/dt = g\ x_1 y_1\ \{h_s\ \rho_e - H\rho_a\}\left\{\prod q_1\ \left[\rho_m + 0.5\{k_x x_1 + k_y y_1\}\right] + (\rho_{m-}\ \rho_f)\varnothing_0\ x_1 y_1 b^{-1}\left(e^{-bz1}-1\right)\right\}^{-1} \quad (17)$$

Consider contrarily that the lithospheric block is under a constant rate of erosion that decreases its height at a rate $h_e = -dz / dt$. Then

$$d(f_{up})\Big/dt = g\ x_1 y_1\ \{H\rho_a - h_s\ \rho_e\}\left\{\prod q_1\ \left[\rho_m + 0.5\{k_x x_1 + k_y y_1\}\right] + (\rho_{m-}\ \rho_f)\varnothing_0\ x_1 y_1 b^{-1}\left(e^{-bz1}-1\right)\right\}^{-1} \quad (18)$$

For a (nearly) constant porosity with depth (Sugai et al. 1994 as just a single example), $b = 0$. Then, Eqs. 11, 13, 17, and 18 simplify significantly and become independent of density of the pore fluid (ρ_f).

Case II This case shows linear increase of density with depth (Z direction) and also the same pattern in two perpendicular horizontal directions X and Y. Siltstones, sandstones, dolostones, and shale from few locations have shown almost linear increase in density with depth up to ~4 km, whereas for overpressured sediments, the relation is strongly non-linear (Fig. 2.7a of Telford et al. 1990). Further, compaction of argillaceous sediments (shale density) increases exponentially up to ~3–4 km depth (Rieke and Chilingarian 1974).

$$\rho(q) = \rho_{m-}(\rho_{m-}\ \rho_f)\varnothing_0 + k_q q \quad (q = x, y, z) \quad (19)$$

$$\text{Therefore, } \rho(x,\ y, z) = \rho_{m-}(\rho_{m-}\ \rho_f)\varnothing_0 + \Sigma k_q q \quad (q = x, y, z) \quad (20)$$

Here, too, the density at the origin (0, 0, 0) is $\rho_m - (\rho_m - \rho_f)\varnothing_0$.

Using the right-hand side expression in Eq. 9, doing triple integration applying limits (0, x_1), (0, y_1), and (0, z_1):

$$\text{Mass of the block is } M = \prod q_1\left\{\rho_{m-}(\rho_{m-}\ \rho_f)\varnothing_0 + 0.5\Sigma k_q q_1\right\} \quad (q = x, y, z) \quad (21)$$

Therefore, the mean density of the block is as follows:

$$\rho_e = \rho_{m-}(\rho_{m-}\ \rho_f)\varnothing_0 + 0.5\Sigma k_q q_1 \quad (q = x, y, z) \tag{22}$$

Isostatic equilibrium demands are as follows:

$$\rho_a\, H = z_1 \rho_e \tag{23}$$

For a constant rate of sedimentation dz/dt = $h_s > 0$, pressure difference per unit time that must drive the lithospheric block down:

$$d(\Delta P)\Big/\mathrm{dt} = g\,\{h_s\,\rho_e - H\rho_a\} \tag{24}$$

The rate of change of the force driving the block to sink is the following:

$$d(F_{down})\Big/\mathrm{dt} = d(\Delta P)\Big/\mathrm{dt} \times x_1 y_1$$
$$= g x_1 y_1 \{h_s \rho_e - H\rho_a\} \tag{25}$$

"$x_1 y_1$"being the horizontal basal area of the block on which the force works.

Dividing this by the mass of the block, as in Eq. 21, the rate of increase of acceleration of the sinking block is as follows:

$$d(f_{down})\Big/\mathrm{dt} = d(F_{down})\Big/\mathrm{dt}\prod q_1^{-1}\rho_e^{-1} \quad (q = x, y, z) \tag{26}$$

$$d(f_{down})\Big/\mathrm{dt} = g z_1^{-1}\{h_s\rho_e - H\rho_a\}\{\rho_{m-}(\rho_{m-}\ \rho_f)\varnothing_0 + 0.5\Sigma k_q q_1\}^{-1} \tag{27}$$
$$(q = x, y, z)$$

$$d(f_{down})\Big/\mathrm{dt} = g z_1^{-1}\left[h_s - H\rho_a\{\rho_{m-}(\rho_{m-}\ \rho_f)\varnothing_0 + 0.5\Sigma k_q q_1\}^{-1}\right] \tag{28}$$
$$(q = x, y, z)$$

Consider contrarily that the lithospheric block is under a constant rate of erosion that decreases its height at a rate h_e = −dz/dt. In this case,

$$d\left(f_{up}\right)\Big/\mathrm{dt}$$
$$= g z_1^{-1}\left[H\rho_a\{\rho_m - (\rho_m - \rho_f)\varnothing_0 + 0.5\ \Sigma k_q q_1\}^{-1} - h_s\right] \tag{29}$$

ρ_f = 0 can be put in Eqs. 21, 28, and 29 to find respective simpler expressions for fluid free "dry" blocks.

Discussions and conclusions

Understanding mean density and isostasy helps to work out the geoid height anomaly, forward seismic modeling, and other geodetic/gravity issues (Fowler 2005). In such seismic modeling, Kirchhoff's integral equation is encountered that involves pressure term (Benthien and Hobbs 2005). From the expression for mass, for case I, in Eq. 11, the pressure exerted on the "xy" area (see Fig. 1) is as follows:

Pressure P_I

$$= \left\{\rho_m \prod q_1 - (\rho_m - \rho_f)\varnothing_0\ b\left(e^{-bz1} + 1\right)\right\} g\, x^{-1} y^{-1} \tag{30}$$

For case II, P_{II}

$$= \prod q_1\ \{\rho_m - (\rho_m - \rho_f)\varnothing_0 + 0.5\ \Sigma k_q q_1\}\ x^{-1} y^{-1} \tag{31}$$

The second byproduct of this study is that one can deduce the Bouguer correction required for gravity station at the top (point M in Fig. 1) of the floating lithosphere. Following Eq. 5.35 of Fowler (2005), the Bouguer correction is as follows:

$$\delta g_B = 2\,\pi\, G\, \rho_e^{/}\, z_s \tag{32}$$

Here, $G = 6.67 \times 10^{-11}$ m^3 kg^{-1} s^{-2}: gravitational constant, z_s: height of the measuring point above the sea level, and $\rho_e^{/}$: mean density of the material between the measurement point (M) and sea level. $\rho_e^{/}$ can be obtained by first finding the mass of the block RSVK in Fig. 1 as follows for both the cases I and II:

$$M_1 = \int_0^{x_1}\int_0^{y_1}\int_{z_s}^{z_1} \rho_{bw}(x, y, z)\ \mathrm{dx\ dy\ dz} \tag{33}$$

This would be followed by

$$\rho_e^{/} = M_1\, g\, x^{-1}\, y^{-1} \tag{34}$$

Isostatic disequilibrium could develop by plate tectonic reasons (Stüwe 2007), or simply by either accumulation (here dz/dt > 0) or removal (here dz/dt < 0) of ice (McGuire 2012). So far geoscientists have deduced isostatic uplift rates (as distance per unit time) from a few places of the world, ranging from a fraction of a millimeter per year (Adams et al. 2010) up to several millimeter per year (Takano et al. 2012). The present work suggests that in geological time scale, however, isostatic disequilibrium should happen by speeding up uplift/subsidence of lithospheric blocks. Sometimes ρ_m and ρ_f are constant at different depths (Syvitski et al. 2007), and in other cases, ρ_f has been reported to increase with depth (Patwardhan 2012). Density of the fluid as well as the matrix must be ideally pressure and therefore depth dependent (Djomani et al. 2001). The presented model presumes depth independent ρ_m and ρ_f magnitudes. Attempting their depth dependence complicate the model (Appendix-I). For clastic rocks/sediments, $\rho_m \sim 2.65$ g cm^{-3} (Cranganu 2009).Compressibility of the pore fluid or water is merely 0.44 (1/GPa). Its thermal expansion coefficient 2×10^{-4} (1/°C) is also low (Zhao et al. 2008). The "formation compressibility" of the bulk porous rocks ranges from 3×10^{-6} to 25×10^{-6} psi (Dandekar 2013), which is too miniscule to contribute significantly in

varying density with depth. In different considerations, the depth dependence of density (ρ_z) can be expressed in ways other than Eq. 3. For example, Ray (2001) presented ρ_z as a function of density of crust at the surface, density and expansion coefficient of the mantle, thickness ratio between the thickened crust and the reference crust, and temperature at depth z. His equation did not consider bulk wet density (ρ_{bw}), matrix density (ρ_m), and fluid density (ρ_f).

This work presumes constant density of asthenosphere (as in Xu et al. 2016 for the North China Craton). For regions with layered asthenosphere of different densities (e.g., Holtzman et al. 2003), the combined pressures exerted by all such layers of known thicknesses can however be easily accommodated in Eq. 9. On the other hand, if we comprehend that the asthenosphere layer is also characterized by smooth linear or exponential variation of density, its mean density can be estimated in the same way it has been done for the lithospheric block (Eq. 12).

Two more issues need to mention. First, sediments undergo compaction at some depth, beyond which obviously pore fluid in determining the mean density of that sediment/sedimentary rock is to be considered zero. Second, if a layer of (nearly) constant density, such as a salt bed, exists at the top or bottom or even inside the density-stratified lithospheric block, the presented equations must be modified. Such a correction would be required when more realistically the lithospheric block consists of a basement of crystalline rock at bottom and sediments/sedimentary rocks over it. The weight exerted by such a layer is to be added along with that of the remainder of the lithospheric slice. Dividing the total weight by the volume of the slice would yield the density (Eq. 12). Rise of buoyant hot magma at sub-surface would disturb the already established density structure considered in this work. The model then would require terrain-specific modification. Density of granite batholithos, possibly lying below sedimentary layers, can vary both vertically and laterally (Bott 1967), which could be systematic due to chemical changes and empirical equations can be set up (Oliver 1977).

Note that vertical brittle fault planes cannot be explained by Anderson's or subsequent other theories of faulting (Misra and Mukherjee 2017). Isostatic disequilibrium (similar to Eq. 28 in the new derivation in this work) could be the favored model in such cases (e.g., Misra et al. 2014, 2015; Mukherjee 2014, 2015).

Acknowledgements This study is supported by research grant of Indian Institute of Technology Bombay. Research sabbatical granted by the Institute to me provided free time to do this work. Internal reviews by Dripta Dutta helped in developing the "Discussions and conclusions" section. Editorial handling by Abdullah M. Al-Amri (Chief Editor) and Eugenio Fazio (Handling Editor) and comments from three anonymous reviewers which have been helpful are also acknowledged.

Appendix-I

The compressibility of the rock matrix, at constant temperature, is as follows:

$$\beta_1 = v_i^{-1}\,\Delta P(v_f - v_i) \tag{35}$$

Here, v_i: initial volume of the matrix, v_f: final volume of the matrix, and ΔP: change in overburden pressure.

Or,

$$\rho_{mz} = \{\rho_{m0}\,(1 + \Delta P\,\beta_1)\} \tag{36}$$

where ρ_{mz}: matrix density at depth z and ρ_{m0}: matrix density at surface.

Pressure at a depth "z" by an overburden rock mass is

$$P = \rho_{ov}\,g\,z \tag{37}$$

ρ_{ov}: Density of the overburden rocks/sediments.

Therefore,

$$\rho_{mz} = \{\rho_{m0}\,(1 + \rho_{ov}\,g\,z\beta_1)\} \tag{38}$$

But ρ_{ov} also depends on ρ_m of the above rocks and eventually on β_1. This work seeks mean density (here ρ_{ov}) so that the pressure exerted by the lithospheric block can be deduced. If we use such an expression of ρ_{mz}, the calculation remains unsolved. The same problem will hold true with ρ_{fz} (density of pore fluid at depth z). A second point is that, compressibility of the matrix and that of the pore fluid at constant pressure, also needs attention. So Eq. 35 alone cannot explain the density of matrix (or the density of fluid from a similar equation) at depth z.

Appendix-II: Symbols

ρ_{bw}: wet bulk density of sediments/rock

ρ_m: matrix/mineral/grain density

ρ_f: fluid density

$\varnothing$: fractional porosity

$\varnothing_z$: porosity at depth z

$\varnothing_0$: porosity at surface

e: exponential series

b: a constant

λ: compaction constant

k_x, k_y, k_z: density gradients along X, Y, and Z directions, respectively

M: mass of lithospheric block

x_1, y_1, z_1: length, width, and thickness of lithospheric block

ρ_e: mean density of lithospheric block

ρ_e': mean density of the material between the measurement point (M) and sea level

ρ_a: density of asthenosphere

H: height of asthenosphere above compensation depth (see Fig. 1)

h_s: sedimentation rate
h_e: erosion rate
ΔP: pressure difference
P_I: pressure in case I
P_{II}: pressure in case II
g: acceleration due to gravity
F_{down}: downward acting force on lithospheric block
f_{down}: downward acting acceleration on lithospheric block
f_{up}: upward acting acceleration on lithospheric block
δg_B: Bouguer gravity correction
G: Gravitational constant
z_s: height of the measuring point above the sea level
β_1: compressibility of rock matrix
v_i: initial volume of matrix
v_f: final volume of matrix
ρ_{mz}: matrix density at depth z
ρ_{m0}: matrix density at surface
ρ_{ov}: density of overburden
ρ_{fz}: density of pore fluid at depth z

References

Adams PN, Opdyke ND, Jaeger JM (2010) Isostatic uplift driven by karstification and sea-level oscillation: modeling landscape evolution in north Florida. Geology 38:531–534. doi:10.1130/G30592.1

Athy LF (1930) Density, porosity, and compaction of sedimentary rocks. AAPG Bull 14:1–22

Benthien GW, Hobbs S (2005) Modeling of sonar transducers and arrays. URL: https://scholar.google.co.in/scholar?hl=en&q=Modeling+of+Sonar+Transducers+and+Arrays+−+gbenthien.net&btnG= (Accessed on 17 Jan 2017)

Bosch GV, Van den Driessche J, Babault J, Robert A, Carballo A, Le Carlier C, Loget N, Prognon C, Wyns R, Baudin T (2016) Peneplanation and lithosphere dynamics in the Pyrenees. Comptes Rendus Géosci 348:194–202. doi:10.1016/j.crte.2015.08.005

Bott MHP (1967) Gravity investigations of subsurface shape and mass distributions of granite batholiths. Geol Soc am Bull 78:859–878. doi:10.1130/0016-7606(1967)78[859:GIOSSA]2.0.CO;2

Bowers GL (2001) Determining an appropriate pore-pressure estimation strategy. In Offshore Technology Conference

Carlson RL, Herrick CN (1990) Densities and porosities in the oceanic crust and their variations with depth and age. J Geophys res 95: 9153–9170

Chaudhuri AK, Sarkar S, Chanda SK (1987) Proterozoic coastal sabkha halite pans: an example from the Pranhita-Godavari Valley, South India. Precamb res 37:305–321. doi:10.1016/0301-9268(87)90080-5

Clark SP Jr, Ringwood AE (1964) Density distribution and constitution of the mantle. Rev Geophys 2:35–87. doi:10.1029/RG002i001p00035

Cordell L (1973) Gravity analysis using an exponential density-depth function—San Jacinto Graben, California. Geophysics 38:684–690. doi:10.1190/1.1440367

Cranganu C (2009) In-situ thermal stimulation of gas hydrates. J pet Sci Eng 65:76–80. doi:10.1016/j.petrol.2008.12.028

Dandekar AY (2013) Petroleum reservoir rock and fluid properties, Second edn. CRC Press, Boca Raton pp. 79. ISBN: 9781439876367

Das BC, Mukherjee BN (1996) Integral calculus—differential equations. UN Dhur & Sons Pvt. Ltd, Kolkata

Djomani YHP, O'Reilly SY, Griffin WL, Morgan P (2001) The density structure of subcontinental lithosphere through time. Earth Planet Sci Lett 184:605–621. doi:10.1016/S0012-821X(00)00362-9

Ebbing J, Braitenberg C, Wienecke S (2007) Insights into the lithospheric structure and tectonic setting of the Barents Sea region from isostatic considerations. Geophys J Int 171:1390–1403. doi:10.1111/j.1365-246X.2007.03602.x

Fowler CMR (2005) The solid Earth: an introduction to global geophysics. Second Edition. Cambridge University Press. ISBN 0 521 58409 4

Goteti G, Ings SJ, Beaumont C (2012) Development of salt minibasins initiated by sedimentary topographic relief. Earth Planet Sci Lett 339-340:103–116. doi:10.1016/j.epsl.2012.04.045

Hofmeister AM, Criss RE (2015) Evaluation of the heat, entropy, and rotational changes produced by gravitational segregation during core formation. J Earth Sci 26:124–133. doi:10.1007/s12583-015-0509-z

Holtzman BK, Kohlstedt DL, Zimmerman ME, Heidelbach F, Hiraga T, Hustoft J (2003) Melt segregation and strain partitioning: implications for seismic anisotropy and mantle flow. Science 301:1227–1230. doi:10.1126/science.1087132

Knapp JH, Knapp CCD, Connor JA, McBride JH, Simmons MD (2007) Deep seismic exploration of the South Caspian Basin: lithosphere-scale imaging of the world's deepest basin. In Yilmaz PO, Isaksen GH (Eds) Oil and gas of the Greater Caspian area: AAPG Studies in Geol 55, 47–49. doi: 10.1306/1205831St553248

Kumar N, Zeyen H, Singh AP (2014) 3D lithosphere density structure of southern Indian shield from joint inversion of gravity, geoid and topography data. J Asian Earth Sci 89:98–107. doi:10.1016/j.jseaes.2014.03.028

Litinsky VA (1989) Concept of effective density: key to gravity depth determinations for sedimentary basins. Geophysics 54:1474–1482. doi:10.1190/1.1442611

Maden N, Aydin A, Kadirov F (2015) Determination of the crustal and thermal structure of the Erzurum-Horasan-Pasinler Basins (eastern Tu¨rkiye) using gravity and magnetic data. Pure Appl Geophys 172: 1599–1614. doi:10.1007/s00024-014-1001-x

Martinec Z, Fullea J (2015) A refined model of sedimentary rock cover in the southeastern part of the Congo basin from GOCE gravity and vertical gravity gradient observations. Int J app Earth Obs Geoinfo 35:70–87. doi:10.1016/j.jag.2014.03.001

Maxant J (1980) Variation of density with rock type, depth, and formation in western Canada basin from density logs. Geophysics 45:1061–1076. doi:10.1190/1.1441107

McCulloh TH (1967) Mass properties of sedimentary rocks and gravimetric effects of petroleum and natural-gas reservoirs, USGS. United States Government Printing Office, Washington

McGuire B (2012) Waking the giant: how a changing climate triggers earthquakes, tsunamis, and volcanoes. Oxford University Press. pp. 1–270. ISBN: 978–0–19-959226-5

Misra AA, Mukherjee S (2017) Dyke-brittle shear relationships in the Western Deccan Strike Slip Zone around Mumbai (Maharashtra, India). In: Mukherjee S, Misra AA, Calvès G, Nemčok M. (Eds) Tectonics of the Deccan Large Igneous Province. Geol Soc, London, Spec Publ 445:269–295. doi: 10.1144/SP445.4

Misra AA, Bhattacharya G, Mukherjee S, Bose N (2014) Near N-S paleo-extension in the western Deccan region in India: does it link strike-slip tectonics with India-Seychelles rifting? Int J Earth Sci 103: 1645–1680. doi:10.1007/s00531-014-1021-x

Misra AA, Sinha N, Mukherjee S (2015) Repeat ridge jumps and microcontinent separation: insights from NE Arabian Sea. Marine Petrol Geol 59:406–428. doi:10.1016/j.marpetgeo.2014.08.019

Motavalli-Anbaran S-H, Zeyen H, Ardestani VE (2013) 3D joint inversion modeling of the lithospheric density structure based on gravity,

geoid and topography data—application to the Alborz Mountains (Iran) and South Caspian Basin region. Tectonophysics 586:192–205. doi:10.1016/j.tecto.2012.11.017

Mukherjee S (2014) Atlas of shear zone structures in meso-scale. Springer Geology. Cham. pp. 1–124. ISBN 978–3–319-0088-6

Mukherjee S (2015) Atlas of structural geology. Elsevier, Amsterdam ISBN: 978-0-12-420152-1

Nemčok M (2016) Rifts and passive margins: structural architecture, thermal regimes, and petroleum systems. Cambridge University Press. ISBN: 978–1–107-02583-7

Oliver HW (1977) Gravity and magnetic investigations of the Sierra Nevada batholith, California. Geol Soc am Bull 88:445–461. doi: 10.1130/0016-7606(1977)88<445:GAMIOT>2.0.CO;2

Patwardhan AM (2012) The dynamic Earth system. Third Edition. PHI Learning Pvt Ltd. pp. 491. ISBN: 978–81–203-4655-0

Pearse J, Bailey RC (2007) Density-contrast instabilities in finite element modelling of slow viscous flow. I J Comp Fluid Dyn 21:121–126. doi:10.1080/10618560701455905

Ray P (2001) From lithospheric thickening and divergent collapse to active continental rifting. In: Miller JA, Holdsworth RE, Buicks RS, Hand M (Eds) Continental reactivation and reworking. Geol Soc London Spec Publ 184:77–88. doi: 10.1144/GSL.SP.2001.184.01.05

Reid I (1987) Crustal structure of the Nova Scotian margin in the Laurentian Channel region. Can J Earth Sci 24:1859–1868. doi:10.1139/e87-176

Rieke HH, Chilingarian CV (1974) Compaction of argillaceous sediments. Elsevier, Amsterdam ISBN: 0-444-41054-6

Román-Sánchez A, Vanwalleghem T, Pena A, Laguna A, Giraldez JV (2017) Controls on soil carbon storage from topography and vegetation in a rocky, semi-arid landscapes. Geoderma. doi:10.1016/j.geoderma.2016.10.013

Romer M-M, Neugebauer NJ (1991) The salt dome problem: a multilayered approach. J Geophys res 96:2389–2396. doi:10.1029/90JB02193

Singh AP, Kumar N, Zeyen H (2015) Three-dimensional lithospheric mapping of the eastern Indian shield: a multi-parametric inversion approach. Tectonophysics 665:164–176. doi:10.1016/j.tecto.2015.09.038

Stüwe K. (2007) Geodynamics of the Lithosphere: An Introduction. Springer. ISBN: 978–3–662-04982-2

Sugai SF, Alperin MJ, Reeburgh WS (1994) Episodic deposition and 137Cs immobility in Skan Bay sediments: a ten-year 210Pb and 137Cs time series. Mar Geol 116:351–372. doi:10.1016/0025-3227(94)90051-5

Syvitski JPM et al. (2007) Prediction of margin stratigraphy. In: Nittrouer CA et al. (Eds) Continental margin sedimentation. Blackwell Publishing. pp. 459–529. ISBN: 978–1–4051-6934-9

Takano Y, Tyler JJ, Kojima H, Yokoyama Y, Tanabe Y, Sato T, Ogawa NO, Ohkouchi N, Fukui M (2012) Holocene lake development and glacial-isostatic uplift at Lake Skallen and Lake Oyako, Lützow-Holm Bay, East Antarctica: based on biogeochemical facies and molecular signatures. Appl Geochem 27:2546–2559. doi:10.1016/j.apgeochem.2012.08.009

Telford WM, Geldart LP, Sheriff RE (1990) Applied Geophysics, Second edn. Cambridge University Press, NewYork pp. 17. ISBN: 0-521-32693-1

Tenzer R, Bagherbandi M, Vajda P (2012) Depth-dependent density change within the continental upper mantle. Contributions to Geophysics and Geodesy. doi:10.2478/v10126-012-0001-z

Turcotte DL, Schubert G (2002) Geodynamics. Cambridge University Press. ISBN: 978–0–521-66186-7

Vanicek P, Krakiwsky EJ (1986) Geodesy: the concepts. Second Edition. North-Holland. Amsterdam. pp. 135. ISBN: 0444 87775 4

Wu J, Mereu RF (1990) The nature of the Kapuskasing Structural Zone: results from the 1984 seismic refraction experiment. In: Salisbury MH, Fountain DM (Eds) Exposed cross-sections of the continental crust. Kluwer Academic Publishers. pp. 563–586. ISBN: 13:978–94–010-6788-1

Xu Y, Zeyen H, Hao T, Santosh M, Li Z, Huang S, Xing J (2016) Lithospheric structure of the North China Craton: integrated gravity, geoid and topography data. Gond res 34:315–323. doi:10.1016/j.gr.2015.03.010

Zhang C, Chen L (1992) Comprehensive study on stability of deep crust and unstable behavior of earthquake source by both failure mechanism and frictional sliding mechanism. Acta Seismol Sinica 5:503–514. doi:10.1007/BF02650545

Zhao C, Hobbs BE, Ord A (2008) Convective and advective heat transfer in geological systems. Springer. pp. 19. ISBN: 978–3–540-79510-0

Zhou Z (2009) 3D vector gravity potential and line integrals for the gravity anomaly of a rectangular prism with 3D variable density contrast. Geophysics 74:143–153. doi:10.1190/1.3239518